Cloning of $p57^{KIP2}$, a cyclin-dependent kinase inhibitor with unique domain structure and tissue distribution

Mong-Hong Lee, Inga Reynisdóttir, and Joan Massagué[1]

Cell Biology and Genetics Program, Howard Hughes Medical Institute, Memorial Sloan-Kettering Cancer Center, New York, New York 10021 USA

Progression through the cell cycle is catalyzed by cyclin-dependent kinases (CDKs) and is negatively controlled by CDK inhibitors (CDIs). We have isolated a new member of the $p21^{CIP1}$/$p27^{KIP1}$ CDI family and named it $p57^{KIP2}$ to denote its apparent molecular mass and higher similarity to $p27^{KIP1}$. Three distinct p57 cDNAs were cloned that differ at the start of their open reading frames and correspond to messages generated by the use of distinct splice acceptor sites. p57 is distinguished from p21 and p27 by its unique domain structure. Four distinct domains follow the heterogeneous amino-terminal region and include, in order, a p21/p27-related CDK inhibitory domain, a proline-rich (28% proline) domain, an acidic (36% glutamic or aspartic acid) domain, and a carboxy-terminal nuclear targeting domain that contains a putative CDK phosphorylation site and has sequence similarity to p27 but not to p21. Most of the acidic domain consists of a novel, tandemly repeated 4-amino acid motif. p57 is a potent inhibitor of G_1- and S-phase CDKs (cyclin E–cdk2, cyclin D2–cdk4, and cyclin A–cdk2) and, to lesser extent, of the mitotic cyclin B–Cdc2. In mammalian cells, p57 localizes to the nucleus, associates with G_1 CDK components, and its overexpression causes a complete cell cycle arrest in G_1 phase. In contrast to the widespread expression of p21 and p27 in human tissues, p57 is expressed in a tissue-specific manner, as a 1.5-kb species in placenta and at lower levels in various other tissues and a 7-kb mRNA species observed in skeletal muscle and heart. The expression pattern and unique domain structure of p57 suggest that this CDI may play a specialized role in cell cycle control.

[*Key Words*: Cell cycle progression; cyclin-dependent kinase; cell cycle inhibitor; domain structure; tissue distribution]

Received January 7, 1995; revised version accepted Feruary 14, 1995.

Cell cycle progression is controlled by cyclin-dependent kinases (CDKs) counterbalanced by CDK inhibitors (CDIs) (for review, see Hunter and Pines 1994; Sherr 1994a). During G_1 phase, these two activities respond in opposite ways to regulatory signals, and the outcome determines whether a cell will complete the division cycle. The best characterized CDKs that control mammalian G_1 progression include the catalytic subunit cdk2 associated with the activating subunit cyclin E and cdk4 or its isoform cdk6 associated with any one of three cyclin D isoforms. These complexes become activated upon phosphorylation of the cdk subunit by CAK (cdk activating kinase), itself a CDK-related kinase complex (Sherr 1994a). A prominent substrate for G_1 CDKs is the retinoblastoma protein Rb (for review, see Hinds and Weinberg 1994; Sherr 1994b). Rb phosphorylation in mid-G_1 phase liberates bound factors including E2F–DP1 heterodimers that are essential for DNA replication. Cdk4 is thought to catalyze a first wave of Rb phosphorylation, whereas cdk2, which is active later in G_1, may help keep Rb and other substrates in the phosphorylated state. These events allow passage through the "Restriction" or "Start" checkpoint beyond which the cell cycle advances on its own, no longer influenced by external signals.

Although regulatory signals can control CDK activity by affecting the expression of CDK components (Matsushime et al. 1991; Cocks et al. 1992; Ewen et al. 1993; Geng and Weinberg 1993), a major venue for CDK regulation by these signals is through the CDIs. The mammalian CDIs described to date fall into two gene families. One family includes $p16^{INK4A}$ (Serrano et al. 1993), $p15^{INK4B}$ (Hannon and Beach 1994), p18, and related proteins of 15–20 kD (Guan et al. 1994; Hannon and Beach 1994), all containing a characteristic fourfold repeated ankyrin-like sequence. The INK4s are specific for cdk4 and cdk6 and appear to compete with cyclin D for binding to these kinases (Serrano et al. 1993). p16 is overexpressed in cells defective in Rb function (Serrano et al. 1993; Li et al. 1994b) and may participate in a feedback

[1]Corresponding author.

loop wherein repression of p16 expression by Rb may allow cdk4 to phosphorylate and inhibit Rb. p15 is upregulated by the antimitogenic cytokine TGF-β in HaCaT human transformed keratinocytes (Hannon and Beach 1994). The *p15* and *p16* genes reside next to each other on human chromosome 9p21, at or near a familial melanoma predisposition locus (Kamb et al. 1994). *p16* is deleted or mutated in a high proportion of primary esophageal squamous cell carcinomas (Mori et al. 1994) and sporadic pancreatic adenocarcinomas (Caldas et al. 1994), substantiating the idea that this is a tumor suppressor gene (Kamb et al. 1994).

The other CDI family includes $p21^{CIP1}$ (aka, WAF1, SDI1, or CAP20) (El-Deiry et al. 1993; Gu et al. 1993; Harper et al. 1993; Xiong et al. 1993; Noda et al. 1994) and $p27^{KIP1}$ (Polyak et al. 1994b; Toyoshima and Hunter 1994), two proteins structurally unrelated to the INK4s. In vitro, p21 and p27 have broad specificity, inhibiting the kinase activity of preactivated cyclin E–cdk2, cyclin D–cdk4, the S-phase CDK cyclin A–cdk2 and, to a lesser extent, the mitotic CDK cyclin B-Cdc2 (Gu et al. 1993; Harper et al. 1993; Xiong et al. 1993; Polyak et al. 1994b; Toyoshima and Hunter 1994). p27 does not inhibit CAK directly (Kato et al. 1994; Nourse et al. 1994), however, it binds to CDK complexes preventing their phosphorylation and activation by CAK (Polyak et al. 1994a,b). When overexpressed in transfected cells, p21 and p27 cause G_1 arrest, suggesting that despite their broad specificity in vitro, these CDIs may act only on G_1 CDKs in vivo (El-Deiry et al. 1993; Harper et al. 1993; Polyak et al. 1994b; Toyoshima and Hunter 1994).

p21 and p27 participate in numerous regulatory responses. The G_1 arrest that follows radiation-induced DNA damage, ostensibly to allow for DNA repair, is mediated by the tumor suppressor p53 that elevates p21 levels transcriptionally, leading to CDK inhibition (El-Deiry et al. 1993, 1994). Mitogen-induced emergence from quiescence occurs with induction of p21 expression, suggesting that cycling cells may need p21 as a regulatory device (Li et al. 1994a; Nourse et al. 1994). In vitro binding of one p21 molecule to a CDK complex stimulates kinase activity, the inhibitory effect appearing only when a second p21 molecule binds to this complex (Zhang et al. 1994). Thus, p21 might act as both a positive and a negative regulator of CDKs in vivo. In addition, p21 but not p27 can inhibit processive DNA replication by binding to proliferating cell nuclear antigen (PCNA), a polymerase δ-subunit (Flores-Rozas et al. 1994; Waga et al. 1994). p27 expression is high in contact-inhibited or mitogen-deprived cells (Polyak et al. 1994a), and, in contrast to p21 expression, it often declines upon mitogen-induced exit from quiescence (Kato et al. 1994; Nourse et al. 1994). Various antimitogens including cAMP in macrophages (Kato et al. 1994) and rapamycin in T-lymphocytes (Nourse et al. 1994) prevent mitogen-induced p27 down-regulation, thus inhibiting CDK activation and G_1 progression. p27 can also act as a passive instrument of antimitogenic action, as in the case of Mv1Lu lung epithelial cells. In these cells, TGF-β down-regulates cdk4 (Ewen et al. 1993), thus lowering the total CDK pool presumably below the threshold imposed by a fixed p27 level (Polyak et al. 1994a).

Despite their recent identification, it is clear that the CDIs play a pivotal role in cell cycle control. Their nature as putative tumor suppressor genes has important implications for diagnosis and treatment of hyperproliferative disorders. Furthermore, the known CDIs are notorious for their structural and functional diversity, suggesting that they may be but the first identified examples of a larger group whose components have highly specialized structure and function. Given this possibility, we searched for additional members of the p21/p27 family. Here, we report the cloning of one such product, $p57^{KIP2}$, and describe its remarkable domain structure, functional properties, and restricted tissue distribution.

Results

Cloning of $p57^{KIP2}$

To identify new members of the $p21^{CIP1}$/$p27^{KIP1}$ family, we screened a mouse embryo cDNA library with a mouse p21 cDNA probe. Restriction analysis of positive cDNA clones from this screening showed that three of them corresponded to a species distinct from p21 and p27. Sequence analysis of one of these clones revealed an open reading frame (Fig. 1A) whose first codon (see Fig. 3, below) is in an optimal context for translation initiation (Kozak 1986). The nucleotide sequence of this open reading frame predicts a product of 348 amino acids with significant sequence similarity to p21 and p27 (Fig. 1A). Most of the similarity is concentrated in a 57-amino-acid domain (residues 30–86) in the amino-terminal region. The corresponding regions in p21 and p27 also show the highest concentration of sequence similarity between these two proteins (Polyak et al. 1994b; Toyoshima and Hunter 1994). When expressed as a recombinant peptide, the corresponding domain from p27 has CDK inhibitory activity (Polyak et al. 1994b), thus defining structurally and functionally this CDI family.

In the newly cloned species, the CDK inhibitory domain is followed by a proline-rich domain, a highly acidic domain, and a carboxy-terminal domain related to p27 (Fig. 1A,B). The proline-rich domain is an 82-amino-acid segment that starts at residue 108 and is 28% proline. This domain contains a consensus mitogen-associated protein (MAP) kinase phosphorylation site (Fig. 1A). The acidic domain is a 107-amino-acid segment that starts at residue 178 and has a 37% glutamic/aspartic acid content. Many of the glutamic residues are found in 19 contiguous repeats of the consensus tetrad sequences Glu-Pro-Val-Glu and Glu-Gln-*X*-*X* (Fig. 1A). The carboxy-terminal domain contains a putative nuclear localization signal and a consensus CDK phosphorylation site, both conserved in p27 together with adjacent sequences (Fig. 1A,B). Thus, the newly cloned species is characterized by a mosaic structure with four distinct domains and a high content in proline and acidic residues (calculated pI = 4.03).

Transcription and translation of this cDNA in vitro

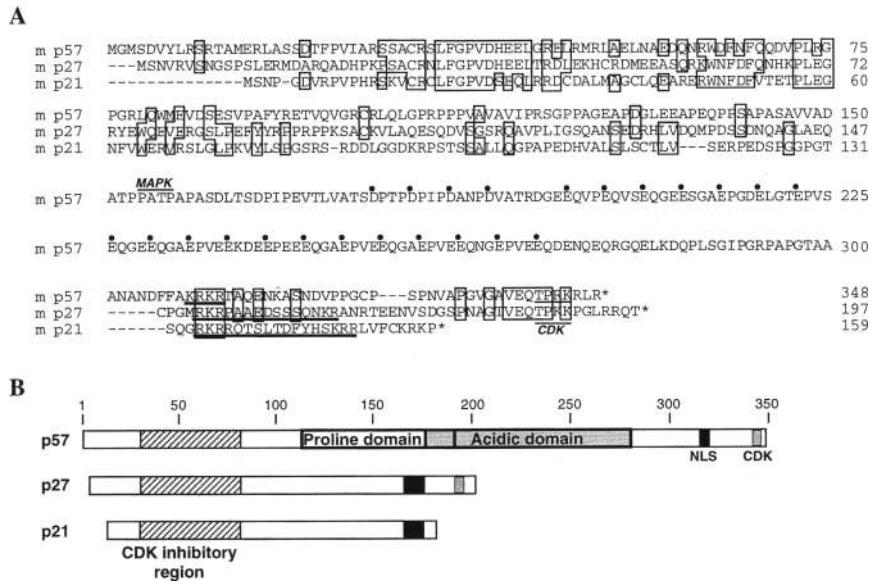

Figure 1. $p57^{KIP2}$ amino acid sequence and comparison with $p27^{KIP1}$ and $p21^{CIP1/WAF1}$. (*A*) Sequence alignment of mouse $p57^{KIP2}$, mouse $p27^{KIP1}$ (Polyak et al. 1994b), and mouse $p21^{CIP1/WAF1}$ (Huppi et al. 1994). Identical amino acids are indicated by boxes. Acidic amino acid residues at the start of tandemly repeated 4-amino-acid motifs are indicated by dots. A putative nuclear localization signals is underlined in each protein. CDK kinase consensus phosphorylation sites in p57 and p27 (CDK) and a MAP kinase consensus phosphorylation site in p57 (MAPK) are indicated. Numbers indicate amino acid residues. (*B*) Schematic representation of p57, p27, and p21 protein domain structures. The three proteins contain a region of similarity (hatched box) that corresponds to the CDK inhibitory domain in p27 (Polyak et al. 1994b). p57 contains a proline-rich domain (open thick box) partially overlapping with an acidic domain (shaded box). Putative nuclear localization signals (NLS; solid boxes) and Cdc2 consensus phosphorylation site (CDK) are indicated. Numbers indicate amino acid residues.

yielded a product that migrated with an apparent molecular mass of 57 kD on SDS electrophoresis gels (Fig. 2). Calculation of this value was based on the migration of coelectrophoresed molecular weight markers and computation with ImageQuant software. To address the discrepancy between this value and a calculated molecular mass of 37.3 kD for the entire open reading frame, we engineered a construct encoding this protein with an influenza virus hemagglutinin (HA) epitope (Meloche et al. 1992) following the carboxy-terminal arginine. When translated in vitro, this construct yielded a specifically immunoprecipitable product migrating at 57 kD on SDS electrophoresis gels (Fig. 2), confirming the value obtained with the unmodified product. Products of the same size were obtained by transfection of mammalian cells with flag–p57 (see Fig. 5A, below), a p57 construct tagged at the amino terminus with the flag epitope (Hopp et al. 1988), or by in vitro translation of flag–p57 (data not shown). We therefore refer to this gene product as $p57^{KIP2}$ following the nomenclature that designates $p27^{KIP1}$ and $p21^{CIP1}$, both of which also migrate larger than predicted on SDS electrophoresis gels.

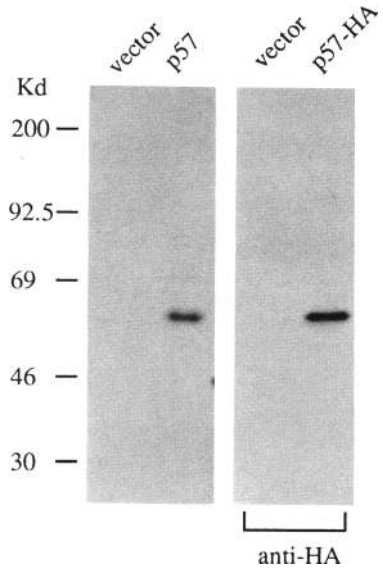

Figure 2. In vitro translation of $p57^{KIP2}$. Vector encoding p57, p57 tagged with the HA epitope at the carboxyl terminus (p57–HA), or empty vector were transcribed in vitro, and the resulting RNA was translated in the presence of [^{35}S]methionine. The entire in vitro translation mixture, or a precipitate with HA antibody (anti-HA), was subjected to SDS-PAGE and fluorography.

Alternative splicing generates amino terminus heterogeneity

Sequence analysis showed that the two other mouse cDNAs isolated in our screen correspond to p57 mRNA forms lacking 38 and 41 bases, respectively, at the 5′ region including the first translation initiator codon (Fig. 3). In both cDNAs, a potential translation initiator codon is located 13 codons downstream of the p57 translation start site, predicting a 335-amino-acid product that we refer to as $p57^{KIP2B}$. PCR amplification of mouse genomic DNA with primers flanking the missing sequence in these cDNAs yielded products that were ~200 bp longer

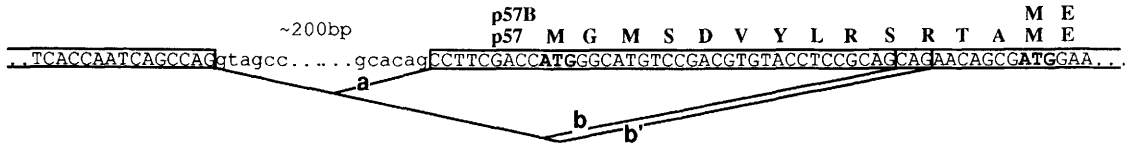

Figure 3. Origin of three p57^{KIP2} cDNA species. Three distinct mouse p57 cDNA clones include the sequence shown in the *left* box continued with sequences shown in the *right* box starting at points designated *a*,*b*, and *b'*, respectively. The remainder of these clones was identical. Two PCR primers flanking the deleted region (see Materials and methods) were used to amplify mouse genomic DNA, yielding a product ~200 bp longer than expected from an intronless genomic region. The ends of the intervening sequence show typical features of an intron including a 5′ splice donor site, $(TC)_n$ tracks (not shown) and a 3′ splice acceptor site. Splicing at positions *b* and *b'* results from the use of alternative acceptor sites. The *b* and *b'* splicing events eliminate a region containing the first methionine codon, which is in an optimal translation initiation context (Kozak 1986) and yield an open reading frame with a potential translation start site 13 amino acids downstream of the start site in full-length p57.

than expected from an intronless genomic sequence. Sequence analysis of the amplified product showed the presence of an intervening sequence flanked by consensus splice sites, suggesting that the three different p57 cDNAs correspond to mRNAs generated by splicing of the same intron with differential use of 3′ splice acceptor sites (Fig. 3).

Nuclear localization

Given the potential antiproliferative activity of p57 in mammalian cells, we studied its expression and activity by transient transfection into the mink lung epithelial cell line R-1B/L17 under conditions that allow >50% of these cells to take up transfected DNA (Attisano et al. 1993; Wrana et al. 1994). Anti–HA immunostaining of cultures expressing a transfected p57–HA demonstrated specific localization of this product in the nucleus with no specific staining discernable in other cellular compartments (Fig. 4 A–D). When transfected into the same cells, a version of this construct truncated at the carboxy-terminal end of the acidic domain (amino acid 281) was expressed in the cytoplasm and excluded from the nucleus (data not shown), suggesting that nuclear localization is specified by the putative nuclear localization signal in the missing domain (Fig. 1). Nuclear localization of p57 was confirmed by anti-flag immunostaining of monkey COS-1 cells overexpressing a transfected flag–p57 construct (Fig. 4 E–H). Examination of the entire stained field suggested that the enlarged morphology of some of the COS-1 nuclei (see Fig. 4F) was not a specific effect of p57 but an effect of cell transfection with the pCMV5 vector used.

CDK interaction in vivo and CDK inhibitory activity in vitro

To identify cellular proteins that interact with p57 in vivo, flag–p57-transfected cells were metabolically labeled with [^{35}S]methionine and cell lysates were precip-

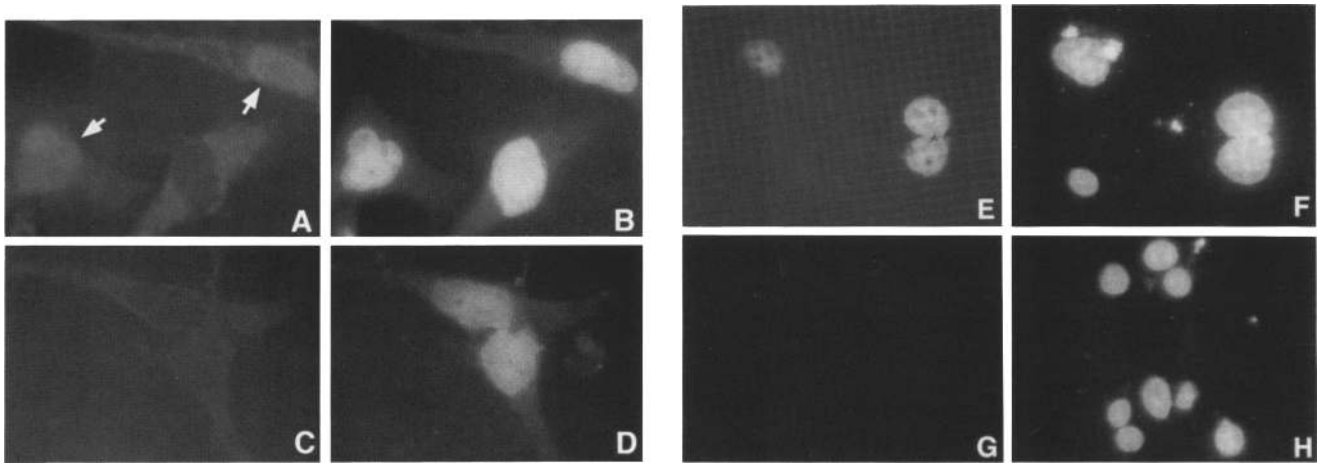

Figure 4. Nuclear localization of p57. R-1B/L17 cells transiently transfected with a p57–HA vector (*A*,*B*) or empty vector (*C*,*D*) were stained with anti-HA mouse monoclonal antibody followed by rhodamine-conjugated anti-mouse immunoglobulin antibody. COS-1 cells transiently transfected with a flag–p57 vector (*E*,*F*) or empty vector (*G*,*H*) were stained with anti-flag mouse monoclonal antibody followed by fluorescein-conjugated anti-mouse immunoglobulin antibody. Indirect immunofluorescence is shown at high magnification (*A*,*C*,*E*,*G*). The same cells were stained with DAPI to visualize nuclear DNA (*B*,*D*,*F*,*H*). Note that two of the cells shown in *A* (arrows) have nuclear staining, whereas cells transfected with empty vector in *C* exclude staining from the nucleus.

itated with flag antibody. This precipitation yielded flag–p57 and various specifically coprecipitating products, as determined by SDS-PAGE (Fig. 5A). To determine whether these products included CDK components, gels containing anti-flag precipitates from unlabeled cells were subjected to immunoblotting with various cyclin and cdk antibodies. The results of these assays demonstrated that p57 specifically coprecipitated with cdk2, cdk4, and cyclins E, A, and D1 (Fig. 5B).

To confirm the ability of p57 to interact with cyclin–cdk complexes and affect their kinase activity, we purified bacterially produced flag-tagged p57 by affinity chromatography on anti-flag beads, added this product to recombinant cyclin–cdk preparations, and assayed their kinase activity. p57 was able to completely inhibit the H1 kinase activity of cyclin E–cdk2 and cyclin A–cdk2 and was 10-fold more potent against these G1 CDKs than against the mitotic CDK cyclin B1–Cdc2 (Fig. 6A,C). Using histone H1 as a substrate, half-maximal inhibition of cyclin E–cdk2 and cyclin A–cdk2 was observed with 0.5 nM p57 (Fig. 6A,C). A similar kinase inhibition pattern was observed using Rb as the substrate for cyclin E–cdk2, cyclin A–cdk2 or cyclin D2–cdk4. When tested in parallel against G_1 CDKs, p57 was reproducibly two- to fivefold more potent than mouse p27 (Fig. 6B,C). In contrast, p57 was less potent than p27 as an inhibitor of cyclin B1–Cdc2 (Fig. 6A,C).

Inhibition of cell entry into S phase

Because p57 was able to interact with CDK components in intact cells and inhibited CDKs in vitro, we tested its ability to inhibit cell cycle progression. For this purpose, a p57 expression vector was transiently transfected into R-1B/L17 cells, and the transfectants were analyzed 48 hr later. As determined by measuring [^{125}I]deoxyuridine incorporation, the relative rate of DNA synthesis at this time was markedly reduced compared with controls transfected with vector alone (Fig. 7). This effect was similar to that caused by transfection of p27 (Fig. 7).

To determine at what point of the cycle these cells were arrested, p57 was cotransfected with the cell surface marker CD16 (Wirthmueller et al. 1992). Forty-eight hours after transfection, cells were stained with anti-CD16 and sorted, and the CD16$^+$ population was subjected to flow cytometry to determine its cell cycle distribution on the basis of DNA content. This analysis demonstrated a striking accumulation of p57-transfected cells in G_1 phase at the expense of both S phase and G_2/M phase (Fig. 7). These results suggest that p57 arrests the cell cycle in G_1 phase.

mRNA expression pattern in human tissues

Northern blot assays with a mouse p57 cDNA probe used at high stringency showed the presence of hybridizing RNA species of 1.5 kb and 7 kb in a limited subset of human tissues (Fig. 8). This is in contrast to the presence of a single p27 mRNA in all these tissues as determined by probing of the same blot with a p27 probe (Fig. 8; Polyak et al. 1994b). The 1.5-kb p57 mRNA species was present at relatively high levels in the placenta and at low levels in skeletal muscle, heart, kidney, and pancreas, was detectable in the brain only after prolonged autoradiographic exposure of the blot, and was not detectable in the lung or liver. Among the tissues tested, the 7-kb species was detectable only in skeletal muscle and heart (Fig. 8) and in two human rhabdomyosarcoma cell lines (data not shown). The relationship between these two mRNA species and the basis for their marked size difference remain to be determined.

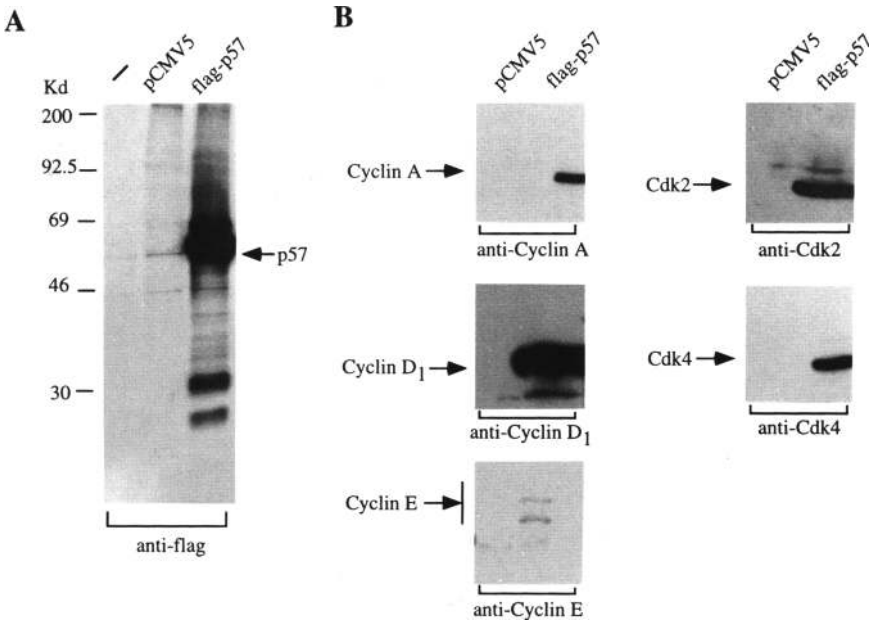

Figure 5. Association of p57 CDK components in mammalian cells. (*A*) R-1B/L17 cells were transiently transfected with empty vector (pCMV5), flag–p57 vector, or were mock transfected (–). Lysates from [^{35}S]-methionine-labeled cells were precipitated with flag antibody and displayed by electrophoresis and fluorography. A specific band of 57 kD corresponding to p57 (arrow) and various specifically coprecipitating bands are observed. (*B*) Cells transiently transfected with empty pCMV5 or flag–p57 vector were lysed and precipited with flag antibody. Immunoprecipitates were resolved by SDS-PAGE and blotted with the indicated antibodies against G_1 CDK components, demonstrating the presence of these components in these p57 precipitates.

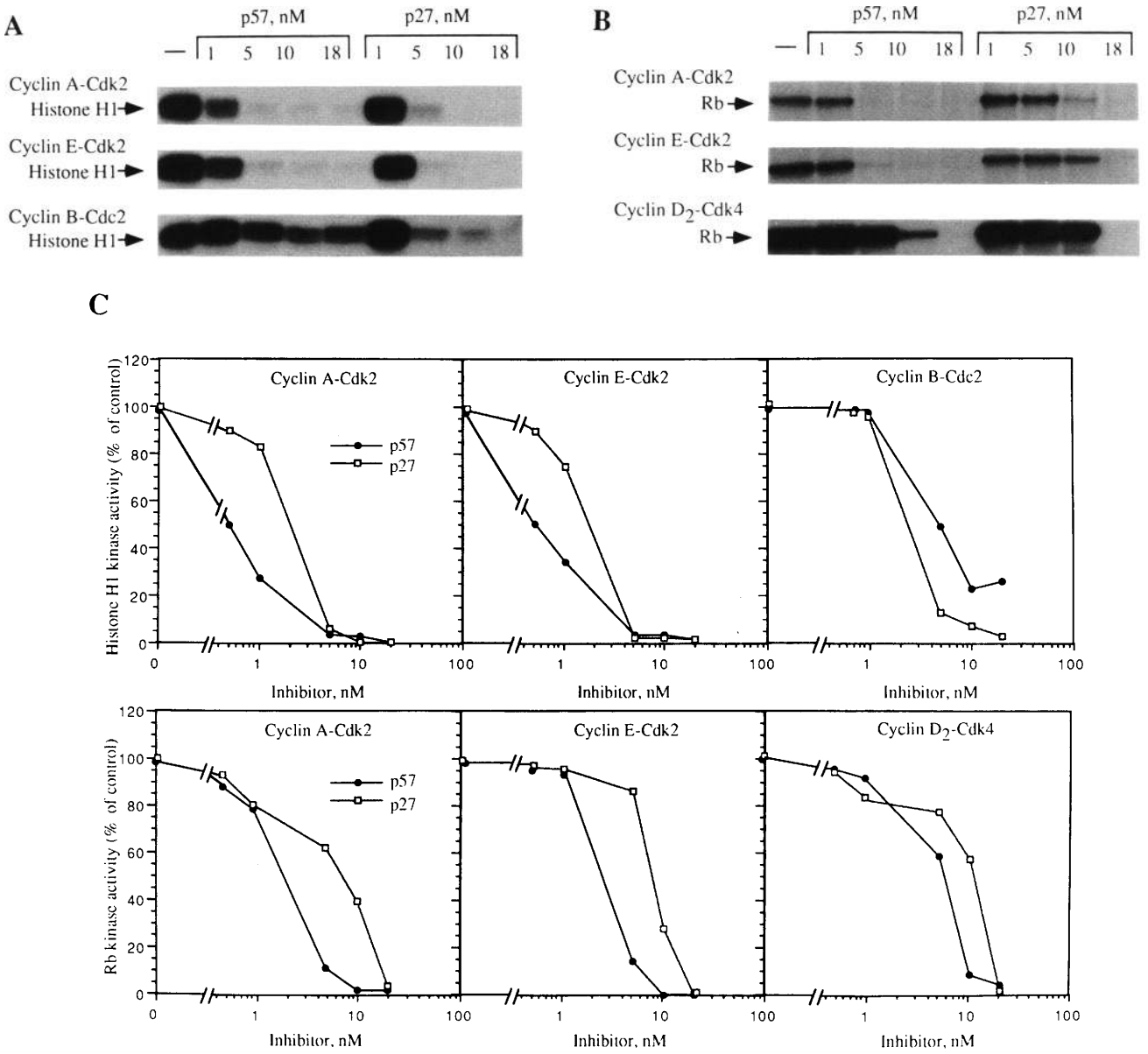

Figure 6. Inhibition of CDK kinase activity in vitro. Insect cell lysates containing the indicated baculovirally expressed cyclin–cdk combinations were assayed for histone H1 kinase activity (*A*) and Rb kinase activity (*B*) in the presence of the indicated concentrations of bacterially produced p57 or p27. Phosphorylation reactions were stopped by boiling in SDS-PAGE sample buffer and resolved by electrophoresis. Autoradiographs show the phosphorylated histone H1 band (*A*) and Rb band (*B*). The signal associated with these bands was quantitated in a PhosphorImager and is plotted (*C*) as percent relative to samples that did not receive inhibitors.

Discussion

We have identified p57^{KIP2}, a new member of the Kip/Cip family of CDK inhibitors that has biochemical and biological activities consistent with a role in negative regulation of G_1 phase in the cell cycle. p57 is distinguished from p21 and p27 by its unique domain structure and distinct tissue distribution pattern. The properties of this novel CDI are indicative of a high degree of diversity in this family of inhibitors.

p57^{KIP2} domain structure

The longest p57 open reading frame predicts a 348-amino-acid protein with a calculated mass of 37.3 kD. However, the products translated from this cDNA in vitro, in *Escherichia coli* and in mammalian cells, migrate on SDS electrophoresis gels as 57-kD proteins. We have confirmed the authenticity of these products by immunoprecipitating recombinant p57 derivatives epitope-tagged at the amino terminus or the carboxyl

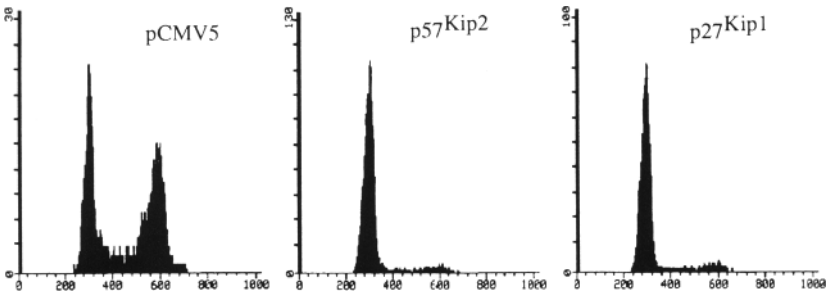

Transfection	%G1	%S	%G2/M	^{125}I-dU(cpm)
pCMV5	37.1	36.7	26.2	1,417±47
p57^{Kip2}	88.7	6.4	4.9	442±21
p27^{Kip1}	88.8	3.7	7.5	437±10

Figure 7. p57 overexpression blocks entry into S phase. R-1B/L17 cells were transiently cotransfected with CD16 and either empty pCMV5 vector, p57 vector, or p27 vector. Two days after transfection, cells were stained with anti-CD16 and the CD16$^+$ population was collected in a cell sorter and subjected to flow cytometry to determine its cell cycle distribution according to DNA content (*Top*). The percent distribution in different cell cycle compartments is shown for each transfectant. [^{125}I]deoxyuridine incorporation assays were done 48 hr post-transfection, and the results are presented as the average ±S.D. of triplicate determinations.

terminus. The anomalous migration of p57 on SDS gels might result from a rigid, elongated shape caused by the high number of prolines in this molecule. p21 and p27 also run anomalously slow on SDS gels, their respective 21- and 27-kD values being larger than their theoretical molecular masses (Harper et al. 1993; Polyak et al. 1994b). Accordingly, we named p57^{KIP2} after its apparent size on SDS gels and also to denote a higher degree of sequence similarity between p57^{KIP2} and p27^{KIP1} than between p57^{KIP2} and p21^{CIP1} (see below).

Three distinct p57 cDNAs that differ at the start of their open reading frames were cloned from a mouse embryo cDNA library. The two smaller cDNAs are missing 38 and 41 bases, repectively, that are present in the larger clone. PCR amplification of mouse genomic DNA with primers that flank the deleted sequences amplified a product consistent with the presence of an ~0.2-kb intron in this region of the gene. Sequence analysis of the amplified product reveals that the three cDNAs correspond to messages generated by the use of distinct splice acceptor sites. The first acceptor site lies 9 bp upstream of the first methionine codon, which is in an optimal context for translation initiation. Use of the other two splice acceptor sites deletes this codon and additional coding region, yielding two nearly identical messages whose first possible translation initiator would yield in both cases a product 13 amino acids shorter than p57 at the amino terminus. We refer to this product as p57^{KIP2B}, or p57B, but have not tested it in inhibition assays or confirmed that it is actually expressed in the cell.

Following this heterogeneous amino-terminal region, the predicted p57 protein sequence has four distinct domains including, in order, a p21/p27-related CDK inhibitory domain, a proline-rich domain, an acidic domain, and a carboxy-terminal nuclear targeting domain. The CDK inhibitory domain is a 57-amino-acid region (residues 30–86) that contains most of the sequence similarity to p21 (36% identity) and p27 (47% identity). The corresponding regions in p21 and p27 also contain most of the sequence similarity (44% identity) between these two proteins (Polyak et al. 1994b; Toyoshima and Hunter 1994). The CDK binding and inhibitory activities of p27 segregate with this region, which retains these activities when produced as a recombinant peptide (Polyak et al. 1994b). Therefore, we infer that the corresponding domains in p21 and p57 contain the CDK inhibitory activity of these proteins. The identification of p57 helps establish this domain as the structural motif defining this CDI family.

The entire p57 portion following the CDK inhibitory domain has a relatively high proline content. However, an 82-amino-acid region extending from residue 108 is particularly proline-rich (28% proline). This domain contains a MAP kinase consensus phosphorylation site. Although we have no evidence that this site is used in vivo, it is worth noting that the CDI Far1 from *Saccharomyces cerevisiae* is phosphorylated by MAP kinases in response to cell stimulation by mating pheromone, this phosphorylation being required for Far1 activation (Peter et al. 1993; Peter and Herskowitz 1994). The p57 proline-rich domain overlaps with an acidic domain that extends from residues 178–284 and is 37% glutamic or aspartic acid. Besides conferring a strongly acidic character to the entire molecule (calculated pI = 4.03), this region is unusual in that its glutamic residues are arranged in 19 contiguous repeats of the tetrapeptide consensus sequences Glu-Pro-Val-Glu and Glu-Gln-*X*-*X*. A search of published sequence data bases did not turn up any other protein with a similar repetitive motif.

No equivalent proline-rich or acidic domains are present in p21 or p27. The presence of these domains in p57, which account for its size difference with p21 and

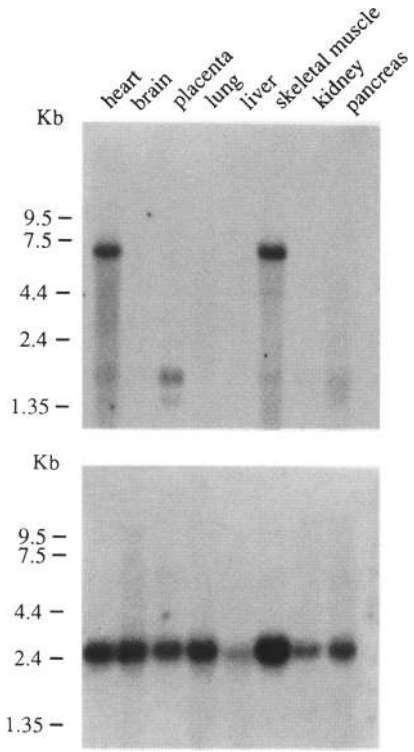

Figure 8. Expression pattern of p57 and p27 in various human tissues. A blot that contains equal amounts of poly(A)$^+$ RNA from the indicated human tissues and was hybridized previously with a p27 cDNA probe (Polyak et al. 1994b; reprinted with permission of the copyright holder, Cell Press) is shown (*bottom*) together with the results of stripping the same blot and reprobing it with a p57 probe (*top*).

p27, may confer the ability to establish specific protein–protein interactions affecting the localization or CDI function of p57 in vivo. Alternatively, these domains could have functions entirely separate from the CDI function. A precedent for the multifunctional nature of these molecules is provided by p21 that has PCNA-dependent DNA polymerase δ inhibitory activity (Flores-Rozas et al. 1994; Waga et al. 1994).

The carboxy-terminal domain of p57 that follows the proline-rich and acidic domains shows sequence similarity to p27. The similarity is clear in two motifs: a putative nuclear localization signal (NLS) and a CDK consensus phosphorylation site. p27 contains a putative bipartite NLS (Polyak et al. 1994b; Toyoshima and Hunter 1994) characterized by two short clusters of basic residues separated by 10 residues (Dingwall and Laskey 1991). The putative NLS in p57 is limited to a KRKR sequence (Boulikas 1993), but its relative position in the molecule and downstream sequence is similar to those of the NLS in p27. Immunostaining of cells transfected with epitope-tagged p57 demonstrated that this protein localizes to the nucleus. Furthermore, a p57 construct missing the carboxy-terminal domain was localized in the cytoplasm and excluded from the nucleus, suggesting that the putative NLS in p57 is functional. The location and adjacent sequence of a consensus CDK phosphorylation site near the carboxyl terminus of p57 are conserved in p27 but not found in p21. These sites might be involved in feedback regulation of p57 and p27 by their target CDKs.

Functional properties and expression pattern of p57^{KIP2}

When purified as a recombinant protein from bacteria and added to kinase assays of recombinant CDK preparations, p57 acts as a potent inhibitor of the G_1 CDKs cyclin E–cdk2 and cyclin D2–cdk4 and the S-phase CDK cyclin A–cdk2. p57 inhibits both Rb and histone H1 phosphorylation by these kinases, and in all our experiments its potency was severalfold higher than that of recombinant p27 produced and assayed in parallel with p57. However, p57 was less potent than p27 as an inhibitor of cyclin B–Cdc2. Preincubation of recombinant CAK (cyclin H–cdk7/MO15 complex; Fisher and Morgan 1994) with p57 did not inhibit the CAK activity of these complexes (J.Y. Kato, C. Sherr, and M.-H. Lee, pers. comm.).

The in vitro activity of p57 suggests that it may act as a CDI primarily in G_1 phase. In support of this possibility, transfection of p57 into Mv1Lu lung epithelial cells induces a profound arrest of the proliferative cycle with accumunlation of cells in G_1. Immunoprecipitation of p57 from these cells retrieves several specifically coprecipitating proteins. Immunoblot assays using appropriate antibodies show that these proteins include cdk2, cdk4, and cyclins E, D1, and A, all of which are important components of the G_1 CDK system. Identification of cell types that express endogenous p57 will be necessary to establish the CDK components that are preferentially targeted by p57 in vivo.

The expression pattern of p57 mRNA in various adult human tissues suggests that its distribution is more restricted than that of p21 and p27, both of which are expressed in most tissues examined (Harper et al. 1993; Polyak et al. 1994b). Two human mRNA species of 1.5 kb and 7 kb, respectively, hybridize with the mouse p57 probe under relatively high stringency conditions. The basis for the size difference between these two messages remains to be determined but may result from differential processing of the p57 transcript or from the existence of different p57-related genes. The 7-kb mRNA is detectable only in skeletal muscle and heart among the tissues that we tested and in human rhabdomyosarcoma cells. The 1.5-kb species is present in placenta and at low levels in the muscle, heart, brain, kidney, and pancreas and was not detected in the lung or liver. Some of these tissues are highly heterogeneous in cellular composition, and their low p57 mRNA levels may reflect expression in only certain cell types.

The present results identify p57 as a putative regulator of G_1 phase. In view of its restricted expression pattern, p57 may function in only certain tissues or cell types. Furthermore, the function of p57 in these tissues may be unique as a result of the unusual protein domains

present in this inhibitor. The availability of its cDNA should allow a further exploration of these questions.

Materials and methods

cDNA cloning and genomic DNA amplification

A λEXlox mouse embryonic cDNA library (Novagen) was screened at low stringency (2× SSC, 0.2% SDS, 25°C) with a mouse p21 cDNA probe generated by PCR based on the published sequence (El-Deiry et al. 1994). Three positive clones were isolated and sequenced. Two of these clones had deletions in the 5′ end when compared with the third one. Two primers (5′-GAGGCCAAGCGTTTCATC-3′ and 5′-CAGGAGCCGTTCATCACC-3′) were designed to amplify by PCR the genomic DNA sequence encompassing the region missing in the smaller cDNA clones. The resulting amplification product was subcloned into pBluescript (Stratagene) and sequenced.

In vitro transcription and translation

A blunt-ended *Eco*RI–*Hin*dIII fragment containing the coding region of the mouse $p57^{KIP2}$ cDNA with or without an influenza virus hemagglutinin HA epitope (Meloche et al. 1992) tagged at the carboxyl terminus was subloned into pET21b (Novagen). These constructs were transcribed in vitro using a commercial kit (Promega) and following the manufacturer's instructions. In vitro translations were performed using Red Nova lysate and accompanying protocol (Novagen). Samples were precipitated with mouse monoclonal anti-HA antibody (12cA5, BAbCO) as described previously (Wrana et al. 1992).

Recombinant $p57^{KIP2}$ and $p27^{KIP1}$

A PCR-generated fragment of the mouse full-length $p57^{KIP2}$ cDNA containing the coding region free of mutations was subloned into the T7 overexpression vector pET21a (Novagen). This construct encodes $p57^{KIP2}$ with a flag epitope (Hopp et al. 1988) at the amino terminus. The protein was expressed in BL21(DE3) pLysS bacteria induced with IPTG. Cells were lysed by sonication in a solution containing 50 mM Tris-HCl (pH 7.4), 500 mM sodium chloride, and 20% glycerol. The lysate was clarified by centrifugation and bound to anti-flag M2 beads (IBI) for 1 hr at 4°C. Recombinant KIP2 was eluted from the beads with 0.2 mg/ml of flag peptide in a buffer containing 150 mM KCl, 50 mM Tris (pH 7.4), 1 mM EDTA, and 20% glycerol. The eluate was aliquoted and stored at −80°C. Recombinant $p27^{KIP1}$ protein was prepared as described previously (Polyak et al. 1994b).

Cell transfection, metabolic labeling and immunoprecipitation

Subclone R-1B/L17 of the Mv1Lu mink lung epithelial cell line (Boyd and Massagué 1989; Attisano et al. 1993) was routinely cultured in MEM supplemented with 10% fetal bovine serum. Cells were transfected with empty pCMV5 vector (Andersson et al. 1989) or this vector encoding p57, p27, or their indicated epitope-tagged derivatives, using the DEAE–dextran transfection method as described previously (Attisano et al. 1993).

For metabolic labeling experiments, cells were transfected with pCMV5 vector alone or encoding flag–p57, a construct encoding $p57^{KIP2}$ tagged at the amino terminus with the flag epitope. Forty-eight hours after transfection, cells were incubated for 30 min in methionine-free medium supplemented with 10% dialyzed fetal bovine serum, followed by incubation in the same medium for 2 hr with 50 μCi/ml of [^{35}S]methionine (Trans^{35}S-label, ICN). Cell pellets were lysed by gentle agitation for 30 min at 4°C in lysis buffer (50 mM Tris-HCl at pH 7.4, 200 mM NaCl, 2 mM EDTA, 0.5% NP-40, 0.3 mM Na-orthovanadate, 50 mM NaF, 80 μM β-glycerophosphate, 20 mM Na-pyrophosphate, 0.5 mM DTT, and protease inhibitors). Lysates were clarified by centrifugation (10,000g for 15 min at 4°C) and immunoprecipitated with flag antibody M2 (IBI).

For protein immunoblotting experiments, cells were transfected with flag–p57. Forty-eight hours after transfection, cells were lysed: the lysates were clarified and precipitated with flag antibody (IBI) in NETN buffer (50 mM NaCl, 50 mM Tris at pH 7.4, 1 mM EDTA, and 0.5% NP-40). The immunoprecipitates were washed four times in NP-40 RIPA buffer, resolved on SDS-PAGE, and electroblotted onto nitrocellulose, and the blots were probed with cyclin E antibody (gift of J. Roberts, Fred Hutchinson Cancer Center, Seattle, WA), cyclin A antibody (UBI), cyclin D1 antibody (UBI), cdk2 antibody (UBI), or cdk4 antibody (PharMingen).

Immunofluorescence analysis

R-1B /L17 cells or COS-1 cells were seeded at a density of 7×10^5 cells per 100 mm dish. Two days later the monolayers were transiently transfected with pCMV5 vector alone or with p57–HA vector or flag–p57 vector as indicated. Twenty-four hours after transfection, 25×10^4 transfected cells were seeded into a single-well tissue culture chamber slide (Nunc). Twenty-four hours later, cells were washed three times with PBS, fixed for 30 min in ice-cold methanol at 4°C, rinsed once with PBS containing 1% Triton X-100, washed three times with PBS, and then incubated for 30 min at room temperature with 1 μg/ml of anti-HA or anti-flag antibody diluted in PBS containing 3% BSA. Cells were then washed four times with PBS and subsequently incubated with 15 μg/ml of donkey antimouse rhodamine-conjugated or fluorescein-conjugated second antibody (Jackson ImmunoResearch Laboratories) diluted in PBS/3% BSA. Cells were then washed four times with PBS, incubated for 5 min at room temperature with 0.1 μg/ml of DAPI (Sigma), washed four times in PBS, and mounted in a solution containing 60% toluene (Cytoseal). Cells were examined by a Zeiss microscope, and the images recorded on Kodak Ektachrome 400.

DNA replication and flow cytometry assays

R-1B/L17 cells were tranfected with mouse $p27^{KIP1}$ vector, $p57^{KIP2}$ vector, or empty pCMV5 vector, and [^{125}I]deoxyuridine incorporation assays were conducted 48 hr after transfection as described previously (Laiho et al. 1990). For flow cytometry assays, cells were transfected with the indicated vectors together with a CD16 vector. Forty-eight hours after transfection, cells were stained with anti-CD16 (Wirthmueller et al. 1992), positive cells were sorted, and their DNA content was analyzed by flow cytometry, all as described previously (Polyak et al. 1994b).

Kinase assays

Baculovirus vectors encoding cyclin A, cyclin B, cyclin E, cyclin D2, cdk2–HA, cdk4, and Cdc2–HA (obtained from C. Sherr, St. Jude Children's Hospital, Memphis, TN, J. Roberts, or H. Piwnica-Worms, Washington University, St. Louis, MO) were used to infect insect H5 cells, and cell lysates were prepared as described previously (Desai et al. 1992). Cell extracts containing baculovirally coexpressed cyclins and cdks were incubated with recombinant $p27^{KIP1}$ or $p57^{KIP2}$ at 37°C for 30 min and precip-

itated with HA antibody, and the precipitates were assayed for histone H1 kinase activity (Koff et al. 1993). Rb kinase activity (Matsushime et al. 1992) was performed as described previously. The level of phosphorylation of the histone H1 and Rb bands were quantitated using PhosphorImager ImageQuant software (Molecular Dynamics).

Northern blots

A blot containing poly(A)$^+$ RNA from various human tissues (Clontech) and hybridized previously with the mouse p27^{KIP1} cDNA (Polyak et al. 1994b) was stripped in heated water containing 0.5% SDS and reprobed with mouse p57^{KIP2} cDNA probe labeled by the random priming method. Hybridization was done at 65°C in a solution containing 1% SDS, 10% dextran sulfate, 0.1 mg/ml of sonicated salmon sperm DNA, and 1 M NaCl and washed in 0.2× SSC and 1% SDS at 65°C for 30 min. A blot containing equivalent amounts of total RNA from human rhabdomyosarcoma cell lines RH18 and RH30 (provided by R. Benezra, Memorial Sloan-Kettering Cancer Center) was probed with mouse p57^{KIP2} cDNA.

Acknowledgments

We are grateful to N. Polyak for assistance with CDK analysis, T. Delohery for flow cytometry assays, J.Y. Kato and C. Sherr for baculoviral vectors and CAK assays, J. Arribas, L. Attisano, N. Polyak, and J. Wrana for valuable advice and discussions, and S. Elledge for communicating unpublished results. This work was supported by the Howard Hughes Medical Institute and by a National Institutes of Health cancer center core grant to Memorial Sloan-Kettering Cancer Center. M.-H.L. and I.R. are Research Associates and J.M. is an Investigator of the Howard Hughes Medical Institute.

The publication costs of this article were defrayed in part by payment of page charges. This article must therefore be hereby marked "advertisement" in accordance with 18 USC section 1734 solely to indicate this fact.

Note

The GenBank data library accession number for the mouse p57 nucleotide sequence reported in this paper is U20553.

References

Andersson, S., D.N. Davis, H. Dahlback, H. Jornvall, and D.W. Russell. 1989. Cloning, structure and expression of the mitochondrial cytochome P-450 sterol 26-hydroxylase, a bile acid biosynthetic enzyme. *J. Biol. Chem.* **264:** 8222–8229.

Attisano, L., J. Cárcamo, F. Ventura, F.M.B. Weis, J. Massagué, and J.L. Wrana. 1993. Identification of human activin and TGF-β type I receptors that form heteromeric kinase complexes with type II receptors. *Cell* **75:** 671–680.

Boulikas, T. 1993. Nuclear localization signals (NLS). *Crit. Revs. Eukar. Gene Expr.* **3:** 193–227.

Boyd, F.T. and J. Massagué. 1989. Growth inhibitory response to transforming growth factor-β linked to expression of a 53 kDa cell surface TGF-β receptor. *J. Biol. Chem.* **274:** 2272–2278.

Caldas, C., S.A. Hahn, L.T. da Costa, M.S. Redston, M. Schutte, A.B. Seymour, C.L. Weinstein, R.H. Hruban, C.J. Yeo, and S.E. Kern. 1994. Frequent somatic mutations and homozygous deletions of the p16 (*MTS1*) gene in pancreatic adenocarcinoma. *Nature Genet.* **8:** 27–32.

Cocks, B.G., G. Vairo, S.E. Bodrug, and J.A. Hamilton. 1992. Supression of growth factor-induced CYL-1 cyclin gene expression by antiproliferative agents. *J. Biol. Chem.* **267:** 12307–12310.

Desai, D., Y. Gu, and D.O. Morgan. 1992. Activation of human cyclin-dependent kinases in vitro. *Mol. Biol. Cell* **3:** 571–582.

Dingwall, C. and R.A. Laskey. 1991. Nuclear targeting sequences: A consensus? *Trends Biochem. Sci.* **16:** 478–481.

El-Deiry, W.S., T. Tokino, V.E. Velculescu, D.B. Levy, R. Parsons, J.M. Trent, D. Lin, E. Mercer, K.W. Kinzler, and B. Vogelstein. 1993. WAF1, a potential mediator of p53 tumor suppression. *Cell* **75:** 817–825.

El-Deiry, W.S., J.W. Harper, P.M. O'Connor, V.E. Velculescu, C.E. Canman, J. Jackman, J.A. Pietenpol, M. Burrell, D.E. Hill, Y. Wang, K.G. Wiman, W.E. Mercer, M.B. Kastan, K.W. Kohn, S.J. Elledge, K.W. Kinzler, and B. Vogelstein. 1994. WAF1/CIP1 is induced in p53-mediated G1 arrest and apoptosis. *Cancer Res.* **54:** 1169–1174.

Ewen, M.E., H.K. Sluss, L.L. Whitehouse, and D.M. Livingston. 1993. TGFβ inhibition of Cdk4 synthesis is linked to cell cycle arrest. *Cell* **74:** 1009–1020.

Fisher, R.P. and D.O. Morgan. 1994. A novel cyclin associates with MO15/CDK7 to form the CDK-activating kinase. *Cell* **78:** 713–724.

Flores-Rozas, H., Z. Kelman, F.B. Dean, Z.-Q. Pan, J.W. Harper, S.J. Elledge, M. O'Donnel, and J. Hurwitz. 1994. Cdk-interacting protein 1 directly binds with proliferating cell nuclear antigen and inhibits DNA replication catalyzed by the DNA polymerase δ holoenzyme. *Proc. Natl. Acad. Sci.* **91:** 8655–8659.

Geng, Y. and R.A. Weinberg. 1993. Transforming growth factor β effects on expression of G1 cyclins and cyclin-dependent protein kinases. *Proc. Natl. Acad. Sci.* **90:** 10315–10319.

Gu, Y., C.W. Turck, and D.O. Morgan. 1993. Inhibition of CDK2 activity in vivo by an associated 20K regulatory subunit. *Nature* **366:** 707–710.

Guan, K.-L., C.W. Jenkins, Y. Li, M.A. Nichols, X. Wu, C.L. O'Keefe, A.G. Matera, and Y. Xiong. 1994. Growth suppression by p18, a p16$^{INK4/MTS1}$ and p14$^{INK4/MTS2}$-related CDK6 inhibitor, correlates with wild-type pRb function. *Genes & Dev.* **8:** 2939–2952.

Hannon, G.J. and D. Beach. 1994. p15^{INK4B} is a potential effector of TGF-β-induced cell cycle arrest. *Nature* **371:** 257–261.

Harper, J.W., G.R. Adami, N. Wei, K. Keyomarsi, and S.J. Elledge. 1993. The p21 cdk-interacting protein CIP1 is a potent inhibitor of G1 cyclin-dependent kinases. *Cell* **75:** 805–816.

Hinds, P. and R.A. Weinberg. 1994. Tumor suppressor genes. *Curr. Opin. Genet. Dev.* **4:** 135–141.

Hopp, T.P., K.S. Prickett, V.L. Price, R.T. Libby, C.J. March, D.P. Cerretti, D.L. Urdal, and P.J. Conlon. 1988. A short polypeptide marker sequence useful for recombinant protein identification and purification. *BioTechnology* **6:** 1204–1210.

Hunter, T. and J. Pines. 1994. Cylins and cancer II: Cyclin D and CDK inhibitiors come of age. *Cell* **79:** 573–582.

Huppi, K., D. Siwarski, J. Dosik, M. Chedid, S. Reed, B. Mock, D. Givol, and J.F. Mushinski. 1994. Molecular cloning, sequencing, chromosomal localization and expression of mouse p21(Waf1). *Oncogene* **9:** 3017–3020.

Kamb, A., N.A. Gruis, J. Weaver-Feldhaus, Q. Liu, K. Harshman, S.V. Tavtigian, E. Stockert, R.S. Day III, B.E. Johnson, and M.H. Skolnick. 1994. A cell cycle regulator potentially involved in genesis of many tumor types. *Science* **264:** 436–440.

Kato, J., M. Matsuoka, K. Polyak, J. Massagué, and C.J. Sherr. 1994. Cyclic AMP-induced G1 phase arrest mediated by an inhibitor (p27KIP1) of cyclin-dependent kinase-4 activation. *Cell* **79:** 487–496.

Koff, A., M. Ohtsuki, K. Polyak, J.M. Roberts, and J. Massagué. 1993. Negative regulation of G1 in mammalian cells: Inhibition of cyclin E-dependent kinase by TGF-β. *Science* **260:** 536–539.

Kozak, M. 1986. Point mutations define a sequence flanking the AUG initiator codon that modulates translation by eukaryotic ribosomes. *Cell* **44:** 283–292.

Laiho, M., J.A. DeCaprio, J.W. Ludlow, D.M. Livingston, and J. Massagué. 1990. Growth inhibition by TGF-β1 linked to suppression of retinoblastoma protein phosphorylation. *Cell* **62:** 175–185.

Li, Y., C.W. Jenkins, M.A. Nichols, and Y. Xiong. 1994a. Cell cycle expression and p53 regulation of the cyclin-dependent kinase inhibitor p21. *Oncogene* **9:** 2261–2268.

Li, Y., M.A. Nichols, J.W. Shay, and Y. Xiong. 1994b. Transcriptional repression of the D-type cyclin-dependent kinase inhibitor p16 by the retinoblastoma susceptibility gene product pRb. *Cancer Res.* **54:** 6078–6082.

Matsushime, H., M.F. Roussel, R.A. Ashnun, and C.J. Sherr. 1991. Colony-stimulation factor 1 regulates novel cyclins during the G1 phase of the cell cycle. *Cell* **65:** 701–713.

Matsushime, H., M.E. Ewen, D.K. Strom, J.-Y. Kato, S.K. Hanks, M.F. Roussel, and C.J. Sherr. 1992. Identification and properties of an atypical catalytic subunit ($p34^{PSK\text{-}J3/cdk4}$) for mammalian D type G1 cyclins. *Cell* **71:** 323–334.

Meloche, S., G. Pages, and J. Pouyssegur. 1992. Functional expression and growth factor activation of an epitope tagged p44 mitogen activated protein kinase, $p44^{mapk}$. *Mol. Biol. Cell.* **3:** 63–71.

Mori, T., K. Miura, T. Aoki, T. Nishihara, S. Mori, and M. Nakamura. 1994. Frequent somatic mutation of MTS1/CDK4I gene in esophageal squamous cell carcinoma. *Cancer Res.* **54:** 3396–3397.

Noda, A., Y. Ning, S.F. Venable, O.M. Pereira-Smith, and J.R. Smith. 1994. Cloning of senescent cell-derived inhibitors of DNA synthesis using an expression screen. *Exp. Cell Res.* **211:** 90–98.

Nourse, J., E. Firpo, M.W. Flanagan, M. Meyerson, K. Polyak, M.-H. Lee, J. Massagué, G.R. Crabtree, and J.M. Roberts. 1994. Rapamycin prevents IL-2-mediated elimination of the cyclin-CDK kinase inhibitor, p27KIP1. *Nature* **372:** 570–573.

Peter, M. and I. Herskowitz. 1994. Direct inhibition of the yeast cyclin-dependent kinase Cdc28-Cln by Far1. *Science* **265:** 1228–1231.

Peter, M., A. Gartner, J. Horecka, G. Ammerer, and I. Herskowitz. 1993. FAR1 links the signal transduction pathway to the cell cycle machinery in yeast. *Cell* **73:** 747–760.

Polyak, K., J.-Y. Kato, M.J. Solomon, C.J. Sherr, J. Massagué, J.M. Roberts, and A. Koff. 1994a. $p27^{KIP1}$, a cyclin–Cdk inhibitor, links transforming growth factor-β and contact inhibition to cell cycle arrest. *Genes & Dev.* **8:** 9–22.

Polyak, K., M.-H. Lee, H. Erdjument-Bromage, A. Koff, P. Tempst, J.M. Roberts, and J. Massagué. 1994b. Cloning of $p27^{KIP1}$ a cyclin-cdk inhibitor and a potential mediator of extracellular antimitogenic signals. *Cell* **78:** 59–66.

Serrano, M., G.J. Hannon, and D. Beach. 1993. A new regulatory motif in cell cycle control causing specific inhibition of cyclin D/ CDK4. *Nature* **366:** 704–707.

Sherr, C.J. 1994a. G1 phase progression: Cycling on cue. *Cell* **79:** 551–555.

———. 1994b. The ins and outs of Rb: Coupling gene expression to the cell cycle clock. *Trends Cell Biol.* **4:** 15–18.

Toyoshima, H. and T. Hunter. 1994. p27, a novel inhibitor of G1 cyclin-Cdk protein kinase activity, is related to p21. *Cell* **78:** 67–74.

Waga, S., G.J. Hannon, D. Beach, and B. Stillman. 1994. The p21 inhibitor of cyclin-dependent kinases controls DNA replication by interaction with PCNA. *Nature* **369:** 574–578.

Wirthmueller, U., T. Kurosaki, M.S. Murakami, and J.V. Ravetch. 1992. Signal transduction by FcδRIII (CD16) is mediated through the δ chain. *J. Exp. Med.* **175:** 1381–1390.

Wrana, J.L., L. Attisano, J. Carcamo, A. Zentella, J. Doody, M. Laiho, X.-F. Wang, and J. Massagué. 1992. TGF-β signals through a heteromeric protein kinase receptor complex. *Cell* **71:** 1003–1014.

Wrana, J.L., L. Attisano, R. Wieser, F. Ventura, and J. Massagué. 1994. Mechanism of activation of the TGF-β receptor. *Nature* **370:** 341–347.

Xiong, Y., G.J. Hannon, H. Zhang, D. Casso, R. Kobayashi, and D. Beach. 1993. p21 is a universal inhibitor of cyclin kinases. *Nature* **366:** 701–704.

Zhang, H., G.J. Hannon, and D. Beach. 1994. p21-containing cyclin kinases exist in both active and inactive states. *Genes & Dev.* **8:** 1750–1758.

Cloning of p57KIP2, a cyclin-dependent kinase inhibitor with unique domain structure and tissue distribution.

M H Lee, I Reynisdóttir and J Massagué

Genes Dev. 1995, **9:**
Access the most recent version at doi:10.1101/gad.9.6.639